



# A new computational scheme for structural static stochastic analysis based on Karhunen–Loève expansion and modified perturbation stochastic finite element method

Zhanjun Shao<sup>1,2</sup> · Xiumei Li<sup>2</sup> · Ping Xiang<sup>1,3</sup>

Received: 29 September 2022 / Accepted: 6 December 2022 / Published online: 21 February 2023  
© The Author(s), under exclusive licence to Springer-Verlag GmbH Germany, part of Springer Nature 2023

## Abstract

Due to uncertainties, deterministic analysis cannot sufficiently reflect the performance of structures. Stochastic analysis can consider the influence of multiple uncertainties factors and improve the confidence of the analysis results. A new stochastic computational scheme, which has the features of Karhunen–Loève (K–L) expansion and modified perturbation stochastic finite element method (MPSFEM), is proposed for the structures with low-level uncertainties, called KL-MPSM for short. The material parameters are regarded as random fields and discretized by K–L expansion. The random variables obtained are substituted into MPSFEM to get the estimates of the first two order moments (mean and variance) of the structural responses. JC method is introduced to compute the reliability indexes and structures failure probability by utilizing the second-order estimates. A deep beam and a plane frame structure are presented as numerical examples to demonstrate the feasibility of KL-MPSM, and some random field properties are studied. The results show that KL-MPSM has good accuracy, efficiency, and advantages in programming. Therefore, KL-MPSM is well suited for static stochastic analysis of structures with low-level uncertainties.

**Keywords** Random field · Karhunen–Loève expansion · Modified perturbation stochastic finite element method · Structural reliability · Stochastic analysis

## 1 Introduction

In order to analyze structures more accurately, the structural uncertainties should be considered [1]. At present, stochastic analysis has been applied to various engineering structures, such as damage of concrete [2,3], rail irregularities in train-bridge coupled vibration system [4,5], lope reliability analysis [6], and some others [7,8]; moreover, in some areas, uncertainty modeling and stochastic approaches are necessary [9]. Random field theory and stochastic finite element method are practical tools for stochastic analysis; therefore,

combining these two approaches to analyze various structures with uncertainties more accurately is meaningful.

Random field theory developed rapidly in the past decades and was widely used. Many studies quantified the stochastic mechanical properties of structures by applying random fields to the material parameters: for instance, Zein [10] quantified the uncertainty in the composite structures by simulating a Gaussian random field over a 3D surface; Rauter [11] proposed a computational modeling approach for short fiber-reinforced composites based on random field theory; Zakian [12] combined stochastic finite cell method and random field theory to analyze the stochastic structures with complex geometries and stochastic material property. The key point of random field theory is how to discretize random fields accurately and quickly. Researchers have proposed many methods for random field discretization, e.g., midpoint method [13], shape function method [1], and spatial average method [14], etc., classified as spatial discretization approaches; expansion optional linear estimation method [15], orthogonal series expansion method [16], Karhunen–Loève series expansion method [17], etc., classified as series

✉ Ping Xiang  
pxiang2-c@my.cityu.edu.hk

<sup>1</sup> School of Civil Engineering, Central South University, Changsha 410075, Hunan, China

<sup>2</sup> School of Civil Engineering and Architecture, Guangxi University, Nanning 530004, Guangxi, China

<sup>3</sup> State Key Laboratory of Hydraulic Engineering Simulation and Safety, Tianjin University, Tianjin, China

expansion approaches. In practical applications, researchers found that the series expansion approaches do not contain the flaws of spatial discretization approaches that there are couplings between the random field discretization and the finite element discretization. Karhunen–Loève expansion is widely applied due to its high efficiency and good accuracy; as shown in Ref. [10–12], they all used K–L expansion. However, it is worth noting that there are also some problems [18]: it is complicated to discretize the random fields with complex geometries and non-stationary non-Gaussian random fields, and the procedures of solving Fredholm integral equation of the second kind are tedious. In order to overcome these problems, researchers have done various types of research: for instance, Zheng [19] improved K–L expansion to discretize random fields with complex geometries and raise the dimensionality to  $n$ -dimensions; Zhang [20] combined wavelet-transform and Galerkin method to propose wavelet-Galerkin method, which can solve Fredholm equation with various types and avoid solving the transcendental equation; for the K–L expansion of non-stationary non-Gaussian random field, Kim [21] and Tong [22] proposed the K–L expansion based on iterative translation approximation method and Linear-moments-based Hermite polynomial model, respectively, and the latter will be more efficient; and there are some similar improvements [23,24]. Then the applicability of K–L expansion is greatly improved. Therefore, this paper introduces K–L expansion as the tool for discretizing random fields.

Various stochastic finite element methods have also been proposed with the development of random field theory. At first, scholars combined the statistic technique with finite element method to propose Monte Carlo finite element method; while the cost of sample computation is too high, it is usually used to verify the accuracy of other methods. Scholars thus began to propose non-sampling approaches, such as perturbation stochastic finite element method (PSFEM) and spectral stochastic finite element method (SSFEM) [17]. PSFEM can obtain the estimates of the first two order moments of the structural response through the low-order Taylor expansion of the governing equation, which reduces the computational cost, but PSFEM is challenging to solve large-variation problems, and dynamic problems and the partial derivatives of the system matrices are necessary. SSFEM combines K–L expansion of random fields and polynomial chaos expansion of structural response to conduct stochastic analysis, and SSFEM does not have those shortcomings of PSFEM, while the introduction of polynomial chaos obviously expands the dimensions of the matrices in the governing equations, which reduces the computational efficiency. The above two methods require modification of the governing equations of FEM; hence they are classified as intrusive approaches. In recent years, non-invasive approaches have become significantly more favored by schol-

ars. The parametric uncertainties processing of this kind of approach is independent of the governing equations of deterministic models, so these non-invasive techniques can eliminate much of the hassle of modifying the deterministic computational scheme. The non-intrusive polynomial chaos expansion is one of the non-invasive approaches, but the existence of the curse of dimensionality [25] makes it somewhat limited; some approaches can alleviate the curse of dimensionality, such as the stochastic collection method [26]. Each of the above methods has its advantages and disadvantages, and scholars have made many improvements to address their shortcomings.

Initially, we wanted to find a method that could efficiently handle static stochastic problems in civil engineering, and this method needed to be easy to program and compute, so PSFEM became the target. The original computational scheme of PSFEM has some problems, and scholars have made some improvements: Kamiński [27–34] has done much research, including the development of  $n$ -order stochastic perturbation technique, and the extension of perturbed stochastic finite element method to statics, thermodynamics, frame structure analysis, metal material analysis, and other fields; Wu [35] proposed a modified computation scheme of PSFEM called modified perturbation stochastic finite element method, which overcomes the flaw of PSFEM that it is necessary to take partial derivatives of system matrices with respect to random variables; meanwhile, MPSFEM can provide results with significantly higher accuracy than PSFEM. MPSFEM is an efficient stochastic analysis tool, and researchers have applied it to stochastic hyperbolic heat conduction problems [36] and running stability analysis of trains [37]. Therefore, we want to promote MPSFEM to random field problems in finite element models and make it possible to calculate structural reliability.

In this paper, MPSFEM and K–L expansion are combined to propose a new computational scheme for static stochastic analysis of engineering structures with random fields. In Sect. 2, a summary of K–L expansion is introduced; In Sect. 3, MPSFEM is described in detail and compared with the original computational scheme of PSFEM, and the advantages of MPSFEM are explained; in Sect. 4, introducing JC method to calculate reliability index and failure probability; in Sect. 5, KL-MPSM is promoted to the plane problem and plane frame structure, and the computational equations are derived in detail; in Sect. 6, four numerical examples are presented, and the results obtained by KL-MPSM are compared with other methods; in Sect. 7, the main research conclusion is summarized, and the subsequent work is envisioned.

## 2 Karhunen–Loève expansion

Assuming that  $X(x, \theta)$  is a one-dimensional (1D) random field on the domain  $\Omega$  ( $x \in \Omega$ ) and probability space  $D$  ( $\theta \in D$ ) with mean  $\bar{X}(x)$  and standard deviation  $\sigma$ . Considering the covariance function of the random field  $C(x_1, x_2)$  is bounded, symmetric, and positive definite, according to Mercer’s theorem [18], it can be expanded as

$$C(x_1, x_2) = \sum_{i=1}^{\infty} \lambda_i f_i(x_1) f_i(x_2), \tag{1}$$

where  $\lambda_i$  and  $f_i(x)$  are the eigenvalue and eigenfunction, respectively, and eigenfunctions are orthogonal and form a complete set; they thus satisfy the following equation.

$$\int_{\Omega} f_i(x) f_j(x) dx = \delta_{ij}, \tag{2}$$

where  $\delta_{ij}$  is the Kronecker-delta function.

From Eq. (1) and considering the orthogonality of eigenfunctions, we can get

$$\int_{\Omega} C(x_1, x_2) f_i(x_2) dx_2 = \lambda_i f_i(x_1). \tag{3}$$

Equation (3) is a homogenous Fredholm integral equation of the second kind, and solving it can yield  $\lambda_i$  and  $f_i(x)$ . Its solution methods include analytical methods [17], numerical methods [20], and the utilizing of discrete sample data [38]. In this paper, a numerical method called wavelet-Galerkin method [20] is introduced.

Then the 1D random field  $X(x, \theta)$  can be expanded to the following form.

$$X(x, \theta) = \bar{X}(x) + \sum_{i=1}^{\infty} \xi_i(\theta) \sqrt{\lambda_i} f_i(x), \tag{4}$$

where  $\xi_i(\theta)$  can be written as

$$\xi_i(\theta) = \frac{1}{\sqrt{\lambda_i}} \int_{\Omega} [X(x, \theta) - \bar{X}(x)] f_i(x) dx; \tag{5}$$

due to the existence of random field  $X(x, \theta)$ ,  $\xi_i(\theta)$  becomes a random variable.

In Eq. (4), the second order properties of  $X(x, \theta)$  are determined by  $\lambda_i$  and  $f_i(x)$ , and the higher order properties are given by  $\xi_i(\theta)$ . If  $X(x, \theta)$  is a Gaussian random field,  $\xi(\theta)$  is a set of standard Gaussian random variables with zero mean and unit variance, and they are uncorrelated. If  $X(x, \theta)$  is a non-Gaussian random field, they may exhibit complex dependencies or correlations that are difficult to determine [39].

## 3 Perturbation stochastic finite element method

### 3.1 The original computational scheme of PSFEM

In the original computational scheme of perturbation stochastic finite element method, it is assumed that the material parameters are random variables and the force is deterministic, the static governing equation can be written as

$$\mathbf{K}(\boldsymbol{\alpha})\mathbf{U}(\boldsymbol{\alpha}) = \mathbf{F}, \tag{6}$$

where  $\boldsymbol{\alpha}$  is a set of variables with zero mean and variance  $\sigma^2$ , and they are relatively small;  $\mathbf{K}(\boldsymbol{\alpha})$ ,  $\mathbf{U}(\boldsymbol{\alpha})$ , and  $\mathbf{F}$  are stochastic stiffness matrix, stochastic displacement vector, and load vector, respectively.

Therefore, the second-order Taylor expansions of  $\mathbf{K}(\boldsymbol{\alpha})$  and  $\mathbf{U}(\boldsymbol{\alpha})$  at their mean value are as follows.

$$\mathbf{K}(\boldsymbol{\alpha}) = \mathbf{K}_0 + \sum_{i=1}^q \mathbf{K}_i^I \alpha_i + \sum_{i=1}^q \sum_{j=i}^q \mathbf{K}_{ij}^{II} \alpha_i \alpha_j + O(\alpha_i^3), \tag{7}$$

$$\mathbf{U}(\boldsymbol{\alpha}) = \mathbf{U}_0 + \sum_{i=1}^q \mathbf{U}_i^I \alpha_i + \sum_{i=1}^q \sum_{j=i}^q \mathbf{U}_{ij}^{II} \alpha_i \alpha_j + O(\alpha_i^3), \tag{8}$$

where  $O(\alpha_i^3)$  denote the third order truncated remainder which satisfies

$$\lim_{x \rightarrow 0} \frac{O(\alpha_i^n)}{\alpha_i^{n-1}} = 0; \tag{9}$$

$q$  is the number of the random variables;  $\mathbf{K}_0$ ,  $\mathbf{K}_i^I$ , and  $\mathbf{K}_{ij}^{II}$  is the mean, first order partial derivative with respect to  $\alpha_i$ , and second order partial derivative with respect to  $\alpha_i, \alpha_j$ , respectively, which can be defined by Eq. (10).

$$\begin{aligned} \mathbf{K}_0 &= \mathbf{K}(\boldsymbol{\alpha})|_{\boldsymbol{\alpha}=0}, \\ \mathbf{K}_i^I &= \left. \frac{\partial \mathbf{K}(\boldsymbol{\alpha})}{\partial \alpha_i} \right|_{\boldsymbol{\alpha}=0}, \\ \mathbf{K}_{ij}^{II} &= \begin{cases} \left. \frac{\partial^2 \mathbf{K}(\boldsymbol{\alpha})}{\partial \alpha_i \partial \alpha_j} \right|_{\boldsymbol{\alpha}=0}, & i \neq j \\ \left. \frac{1}{2} \frac{\partial^2 \mathbf{K}(\boldsymbol{\alpha})}{\partial \alpha_i^2} \right|_{\boldsymbol{\alpha}=0}, & i = j, \end{cases} \end{aligned} \tag{10}$$

and  $\mathbf{U}_0$ ,  $\mathbf{U}_i^I$ , and  $\mathbf{U}_{ij}^{II}$  have the same form as Eq. (10).

Since  $\mathbf{U}_0$ ,  $\mathbf{U}_i^I$ , and  $\mathbf{U}_{ij}^{II}$  cannot be directly calculated; we need to substitute Eqs. (7–10) into Eq. (6) and corresponding the terms in order, then we have:

$$\mathbf{K}_0 \mathbf{U}_0 = \mathbf{F}, \tag{11}$$

$$\mathbf{U}_i^I = -\mathbf{K}_0^{-1} \mathbf{K}_i^I \mathbf{U}_0, \quad (12)$$

$$\mathbf{U}_{ij}^{II} = \mathbf{K}_0^{-1} \left( -\mathbf{K}_i^I \mathbf{U}_j^I - \mathbf{K}_j^I \mathbf{U}_i^I - \mathbf{K}_{ij}^{II} \mathbf{U}_0 \right), \quad (j < i), \quad (13)$$

$$\mathbf{U}_{ii}^{II} = \mathbf{K}_0^{-1} \left( -\mathbf{K}_i^I \mathbf{U}_i^I - \mathbf{K}_{ii}^{II} \mathbf{U}_0 \right), \quad (j = i), \quad (14)$$

where,  $\mathbf{U}_0$  is the deterministic displacement vector;  $\mathbf{U}_i^I$  and  $\mathbf{U}_{ij}^{II}$  (when  $i = j$ ,  $\mathbf{U}_{ij}^{II} = \mathbf{U}_{ii}^{II}$ ) denote the first order and second order perturbation of the displacement vector, respectively.

Through Eq. (8) and combined with Eqs. (11–14), we can obtain the mean vector  $E(\mathbf{U}(\boldsymbol{\alpha}))$  and covariance matrix  $\text{Cov}(\mathbf{U}(\boldsymbol{\alpha}))$  of the structural displacement by Eqs. (15) and (16).

$$E(\mathbf{U}(\boldsymbol{\alpha})) = \mathbf{U}_0 + \sum_{i=1}^q \sum_{j=i}^q \mathbf{U}_{ij}^{II} \sigma_i \sigma_j \rho_{ij} + \left( \|\boldsymbol{\sigma}\|_{\infty}^3 \right), \quad (15)$$

$$\text{Cov}(\mathbf{U}(\boldsymbol{\alpha}), \mathbf{U}) = \sum_{i=1}^q \sum_{j=1}^q \mathbf{U}_i^I \mathbf{U}_j^{IT} \rho_{ij} \sigma_i \sigma_j + \left( \|\boldsymbol{\sigma}\|_{\infty}^3 \right), \quad (16)$$

where  $\|\boldsymbol{\sigma}\|_{\infty}$  is the infinite norm of  $\boldsymbol{\sigma}$ ;  $\rho_{ij} = \frac{\text{Cov}(\alpha_i, \alpha_j)}{\sigma_i \sigma_j}$ . If the random variables are uncorrelated, Eqs. (15) and (16) can be rewritten as

$$E(\mathbf{U}(\boldsymbol{\alpha})) = \mathbf{U}_0 + \sum_{i=1}^q \mathbf{U}_{ii}^{II} \sigma_i^2 + \left( \|\boldsymbol{\sigma}\|_{\infty}^3 \right), \quad (17)$$

$$\text{Cov}(\mathbf{U}(\boldsymbol{\alpha}), \mathbf{U}(\boldsymbol{\alpha})) = \sum_{i=1}^q \mathbf{U}_i^I \mathbf{U}_i^{IT} \sigma_i^2 + \left( \|\boldsymbol{\sigma}\|_{\infty}^3 \right). \quad (18)$$

From the equations of the original computational scheme of perturbation stochastic finite element method, we can know that:

- (1) PSFEM is mainly suitable for the case of low-level variation (the coefficient of variation is usually set around 10% ~ 15%).
- (2) The computational cost and accuracy of PSFEM increase with the items in Eq. (8).
- (3) The first and second order partial derivatives of the stiffness matrix ( $\mathbf{K}_i^I$  and  $\mathbf{K}_{ij}^{II}$ ) are necessary.

These features are also the drawbacks of PSFEM.

### 3.2 Modified perturbation stochastic finite element method

In engineering structures, uncertainties in material properties often manifest themselves as non-Gaussian [40,41], while the Gaussian assumption is still applied due to its simplicity and the lack of relevant experimental data [39,41–43].

Therefore, to facilitate the verification of the accuracy and equation derivation of MPSFEM, the random fields mentioned in the following sections of this paper are all Gaussian random fields.

Depending on the correlation between random variables, Wu [35] classified MPSFEM into three cases, including uncorrelated random variables, uncorrelated random variables with a symmetric joint probability density function (PDF), and correlated random variables. As described in Sect. 2, if the random field is Gaussian,  $\boldsymbol{\xi}(\theta)$  is a set of uncorrelated standard Gaussian random variables with zero mean and unit variance, and it is clear that the joint PDF of  $\boldsymbol{\xi}(\theta)$  is symmetric and Gaussian. Therefore, we only discuss the first and second cases.

If the random variables are uncorrelated,  $\mathbf{U}_i^I$  and  $\mathbf{U}_{ij}^{II}$  must be calculated through Eqs. (11)–(14), then substituting  $\mathbf{U}_{ij}^{II} \sigma_i \sigma_j$  and  $\mathbf{U}_i^I \sigma_i$  into Eqs. (15) and (16) to get the second-order estimates of  $\mathbf{U}(\boldsymbol{\alpha})$ . However, in MPSFEM,  $\mathbf{U}_{ij}^{II} \sigma_i \sigma_j$  and  $\mathbf{U}_i^I \sigma_i$  can be calculated directly by another technique.

The third-order Taylor expansion of  $\mathbf{U}(\boldsymbol{\alpha})$  at the mean can be written as

$$\begin{aligned} \mathbf{U}(\boldsymbol{\alpha}) = & \mathbf{U}_0 + \sum_{i=1}^q \mathbf{U}_i^I \alpha_i + \sum_{i=1}^q \sum_{j=i}^q \mathbf{U}_{ij}^{II} \alpha_i \alpha_j \\ & + \sum_{i=1}^q \sum_{j=i}^q \sum_{k=j}^q \mathbf{U}_{ijk}^{III} \alpha_i \alpha_j \alpha_k + \left( \|\boldsymbol{\sigma}\|_{\infty}^4 \right). \end{aligned} \quad (19)$$

Hence, for the case of uncorrelated random variables, the third-order estimate of the mean vector and covariance matrix of  $\mathbf{U}(\boldsymbol{\alpha})$ , imitating Eqs. (17) and (18), can be expressed as

$$\begin{aligned} E(\mathbf{U}(\boldsymbol{\alpha})) = & \mathbf{U}_0 + \sum_{i=1}^q \mathbf{U}_{ii}^{II} \sigma_i^2 \\ & + \sum_{i=1}^q \sum_{j=i}^q \sum_{k=j}^q \mathbf{U}_{ijk}^{III} \sigma_i \sigma_j \sigma_k \rho_{ijk} + \left( \|\boldsymbol{\sigma}\|_{\infty}^4 \right), \end{aligned} \quad (20)$$

$$\begin{aligned} \text{Cov}(\mathbf{U}(\boldsymbol{\alpha}), \mathbf{U}(\boldsymbol{\alpha})) = & \sum_{i=1}^q \mathbf{U}_i^I \mathbf{U}_i^{IT} \\ & + \sum_{k=1}^q \sum_{i=1}^q \sum_{j=i}^q \mathbf{U}_k^I \sigma_k \mathbf{U}_{ij}^{II T} \sigma_i \sigma_j \rho_{ijk} \\ & + \sum_{i=1}^q \sum_{j=i}^q \sum_{k=1}^q \mathbf{U}_{ij}^{II} \sigma_i \sigma_j \mathbf{U}_k^T \sigma_k \rho_{ijk} + \left( \|\boldsymbol{\sigma}\|_{\infty}^4 \right), \end{aligned} \quad (21)$$

where

$$\rho_{ijk} = \frac{E(\alpha_i \alpha_j \alpha_k)}{\sigma_i \sigma_j \sigma_k}. \quad (22)$$

Defining a deterministic vector  $\mathbf{a}_s$  by

$$\mathbf{a}_s = \left( \underbrace{0, \dots, 0}_{s-1}, \sigma_s, \underbrace{0, \dots, 0}_{q-s} \right), \tag{23}$$

where  $\sigma_s$  is the standard deviation of  $\alpha_s$ .

Replacing the random vector  $\boldsymbol{\alpha}$  in Eq. (20) with the deterministic vectors  $\pm \mathbf{a}_s$ , we have

$$\begin{aligned} \mathbf{U}(\mathbf{a}_s) &= \mathbf{U}_0 + \mathbf{U}_s^I \sigma_s + \mathbf{U}_{ss}^{II} \sigma_s^2 + \mathbf{U}_{sss}^{III} \sigma_s^3 \\ &\quad + \left( \|\boldsymbol{\sigma}\|_\infty^4 \right), \end{aligned} \tag{24}$$

$$\begin{aligned} \mathbf{U}(-\mathbf{a}_s) &= \mathbf{U}_0 - \mathbf{U}_s^I \sigma_s + \mathbf{U}_{ss}^{II} \sigma_s^2 - \mathbf{U}_{sss}^{III} \sigma_s^3 \\ &\quad + \left( \|\boldsymbol{\sigma}\|_\infty^4 \right). \end{aligned} \tag{25}$$

By adding Eqs. (24) and (25), and subtracting Eq. (25) from Eq. (24), we can obtain  $\mathbf{U}_{ss}^{II} \sigma_s^2$  and  $\mathbf{U}_s^I \sigma_s$  directly by the following equations.

$$\mathbf{U}_{ss}^{II} \sigma_s^2 = \frac{z_s}{2} + \left( \|\boldsymbol{\sigma}\|_\infty^4 \right), \tag{26}$$

$$\mathbf{U}_s^I \sigma_s = \frac{w_s}{2} + \left( \|\boldsymbol{\sigma}\|_\infty^3 \right), \tag{27}$$

where

$$z_s = \mathbf{U}(\mathbf{a}_s) + \mathbf{U}(-\mathbf{a}_s) - 2\mathbf{U}_0, \tag{28}$$

$$w_s = \mathbf{U}(\mathbf{a}_s) - \mathbf{U}(-\mathbf{a}_s), \tag{29}$$

and from Eqs. (24–25), and (28–29), we can know that

$$w_i = O\left(\|\boldsymbol{\sigma}\|_\infty^1\right), \quad z_i = O\left(\|\boldsymbol{\sigma}\|_\infty^2\right). \tag{30}$$

Therefore, through Eqs. (26), (27) and (30), we can get several parts of Eqs. (20) and (21)

$$\mathbf{U}_s^I \mathbf{U}_s^{IT} \sigma_s^2 = \frac{1}{4} w_s w_s^T + O\left(\|\boldsymbol{\sigma}\|_\infty^4\right), \tag{31}$$

$$\mathbf{U}_s^I \mathbf{U}_{ss}^{IIT} \sigma_s^3 = \frac{1}{4} w_s z_s^T + O\left(\|\boldsymbol{\sigma}\|_\infty^5\right). \tag{32}$$

Substituting Eqs. (27), (31) and (32) into Eqs. (20) and (21), we have

$$\mathbf{E}(\mathbf{U}(\boldsymbol{\alpha})) = \mathbf{U}_0 + \frac{1}{2} \sum_{s=1}^q z_s + O\left(\|\boldsymbol{\sigma}\|_\infty^3\right), \tag{33}$$

$$\begin{aligned} \text{Cov}(\mathbf{U}(\boldsymbol{\alpha}), \mathbf{U}(\boldsymbol{\alpha})) &= \sum_{s=1}^q \frac{1}{4} w_s w_s^T \\ &\quad + \sum_{s=1}^q \frac{1}{4} w_s z_s^T \rho_{sss} + \sum_{s=1}^q \frac{1}{4} z_s w_s^T \rho_{sss} \\ &\quad + \sum_{k=1(k \neq i)}^q \sum_{i=1}^q \sum_{j=i}^q \mathbf{U}_k^I \sigma_k \mathbf{U}_{ij}^{IIT} \sigma_i \sigma_j \rho_{ijk} \end{aligned}$$

$$+ \sum_{i=1}^q \sum_{j=i}^q \sum_{k=1(k \neq i)}^q \mathbf{U}_{ij}^{II} \sigma_i \sigma_j \mathbf{U}_k^I \sigma_k \rho_{ijk} + \left( \|\boldsymbol{\sigma}\|_\infty^4 \right), \tag{34}$$

and Eq. (34), due to  $z_s z_s^T = O\left(\|\boldsymbol{\sigma}\|_\infty^4\right)$ , can be rewritten as

$$\begin{aligned} \text{Cov}(\mathbf{U}(\boldsymbol{\alpha}), \mathbf{U}(\boldsymbol{\alpha})) &= \frac{1}{4} \sum_{s=1}^q (w_s + z_s \rho_{sss})(w_s + z_s \rho_{sss})^T + O\left(\|\boldsymbol{\sigma}\|_\infty^3\right). \end{aligned} \tag{35}$$

In this way, it is possible to obtain the mean vector and covariance matrix of  $\mathbf{U}(\boldsymbol{\alpha})$  without taking the partial derivative of  $\mathbf{K}(\boldsymbol{\alpha})$  with respect to  $\alpha_i$ . Meanwhile, Eqs. (34) and (35) incorporate some terms beyond the second order that do not exist in Eqs. (17) and (18), which makes MPSFEM more accurate than the original scheme of PSFEM.  $\mathbf{U}(\pm \mathbf{a}_s)$  are the keys to solving the above equations, which can be calculated easily by

$$\mathbf{K}(\pm \mathbf{a}_s) \mathbf{U}(\pm \mathbf{a}_s) = \mathbf{F}. \tag{36}$$

Obviously, Eq. (36) does not change the governing equation of FEM; it just replaces the random vector  $\boldsymbol{\alpha}$  in the stochastic stiffness matrix  $\mathbf{K}(\boldsymbol{\alpha})$  with the deterministic vector  $\pm \mathbf{a}$ . This approach allows direct use of the original finite element program, significantly saving programming time.

For the standard Gaussian random variables obtained by K–L expansion, MPSFEM can provide higher accuracy. If the random variables are uncorrelated and have a symmetric joint PDF [35], there are some properties:

$$\begin{aligned} \mathbf{E}(\alpha_i \alpha_j \alpha_k) &= 0, \\ \mathbf{E}(\alpha_i \alpha_j \alpha_k \alpha_l) &= \begin{cases} \mathbf{E}(\alpha_i^2 \alpha_k^2) & i = j, k = l \\ 0 & \text{other} \end{cases}, \\ \text{Cov}(\alpha_i, \alpha_j \alpha_k) &= \text{Cov}(\alpha_i \alpha_j, \alpha_k) = 0, \\ \text{Cov}(\alpha_i \alpha_j \alpha_k, \alpha_l) &= \mathbf{E}(\alpha_i \alpha_j \alpha_k \alpha_l), \\ \text{Cov}(\alpha_i \alpha_j, \alpha_k \alpha_l) &= \begin{cases} \mathbf{E}(\alpha_i^2 \alpha_k^2) - \mathbf{E}(\alpha_i^2) \mathbf{E}(\alpha_k^2) & i = j, k = l \\ \mathbf{E}(\alpha_i^2 \alpha_j^2) & i = k, j = l, i \neq j \\ 0 & \text{other} \end{cases}. \end{aligned} \tag{37}$$

The fourth-order Taylor expansion of  $\mathbf{U}(\boldsymbol{\alpha})$  at the mean can be written as

$$\begin{aligned} \mathbf{U}(\boldsymbol{\alpha}) &= \mathbf{U}_0 + \sum_{i=1}^q \mathbf{U}_i^I \alpha_i + \sum_{i=1}^q \sum_{j=i}^q \mathbf{U}_{ij}^{II} \alpha_i \alpha_j \\ &\quad + \sum_{i=1}^q \sum_{j=i}^q \sum_{k=j}^q \mathbf{U}_{ijk}^{III} \alpha_i \alpha_j \alpha_k \end{aligned}$$

$$\begin{aligned}
 & + \sum_{i=1}^q \sum_{j=i}^q \sum_{k=j}^q \sum_{l=k}^q \mathbf{U}_{ijkl}^{IV} \alpha_i \alpha_j \alpha_k \alpha_l \\
 & + \left( \|\boldsymbol{\alpha}\|_\infty^5 \right). \tag{38}
 \end{aligned}$$

Therefore, for the case of uncorrelated random variables with a symmetric joint PDF, the third-order estimate of the mean vector and covariance matrix of  $\mathbf{U}(\boldsymbol{\alpha})$  can be expressed as

$$\begin{aligned}
 \mathbf{E}(\mathbf{U}) & = \mathbf{U}_0 + \sum_{i=1}^q \mathbf{U}_{ii}^{\text{II}} \sigma_i^2 + \sum_{i=1}^q \mathbf{U}_{iii}^{IV} \sigma_i^4 \rho_{iii} \\
 & + \sum_{i=1}^q \sum_{j=i+1}^q \mathbf{U}_{ijj}^{IV} \sigma_i^2 \sigma_j^2 \rho_{ijj} + O\left(\|\boldsymbol{\sigma}\|_\infty^5\right), \tag{39}
 \end{aligned}$$

$$\begin{aligned}
 \text{Cov}(\mathbf{U}(\boldsymbol{\alpha}), \mathbf{U}(\boldsymbol{\alpha})) & = \sum_{i=1}^q \left( \mathbf{U}_i^I \mathbf{U}_i^{IT} \sigma_i^2 \right. \\
 & + \mathbf{U}_{iii}^{\text{III}} \mathbf{U}_i^{IT} \sigma_i^4 \rho_{iii} + \mathbf{U}_i^I \mathbf{U}_{iii}^{\text{III}T} \sigma_i^4 \rho_{iii} \left. \right) \\
 & + \sum_{i=1}^q \sum_{j=1}^q \mathbf{U}_{ii}^{\text{II}} \mathbf{U}_{jj}^{\text{II}T} \sigma_i^2 \sigma_j^2 (\rho_{ijj} - 1) \\
 & + \sum_{i=1}^q \sum_{j=i+1}^q \left( \mathbf{U}_i^I \mathbf{U}_{ijj}^{\text{III}T} \sigma_i^2 \sigma_j^2 + \mathbf{U}_{ijj}^{\text{III}} \mathbf{U}_i^{IT} \sigma_i^2 \sigma_j^2 \right) \rho_{ijj} \\
 & + \sum_{i=1}^q \sum_{j=i+1}^q \left( \mathbf{U}_j^I \mathbf{U}_{ijj}^{\text{III}T} \sigma_i^2 \sigma_j^2 + \mathbf{U}_{ijj}^{\text{III}} \mathbf{U}_j^{IT} \sigma_i^2 \sigma_j^2 \right) \\
 & + \mathbf{U}_{ii}^{\text{II}} \mathbf{U}_{ii}^{\text{II}T} \sigma_i^2 \sigma_j^2 \rho_{ijj} + O\left(\|\boldsymbol{\sigma}\|_\infty^5\right), \tag{40}
 \end{aligned}$$

where

$$\rho_{ijkl} = \frac{\mathbf{E}(\alpha_i \alpha_j \alpha_k \alpha_l)}{\sigma_i \sigma_j \sigma_k \sigma_l}. \tag{41}$$

Defining a deterministic vector  $\mathbf{b}_s$  by

$$\mathbf{b}_s = \left( \underbrace{0, \dots, 0}_{s-1}, \sqrt{\rho_{ssss}} \sigma_s, \underbrace{0, \dots, 0}_{q-s} \right). \tag{42}$$

Replacing the random vector  $\boldsymbol{\alpha}$  in Eq. (38) with the deterministic vectors  $\pm \mathbf{b}_s$ , we have

$$\begin{aligned}
 \mathbf{U}(\mathbf{b}_s) & = \mathbf{U}_0 + \mathbf{U}_s^I \sigma_s \rho_s^{\frac{1}{2}} + \mathbf{U}_{ss}^{\text{II}} \sigma_s^2 \rho_{ssss} \\
 & + \mathbf{U}_{sss}^{\text{III}} \sigma_s^3 \rho_{ssss}^{\frac{3}{2}} + \mathbf{U}_{ssss}^{IV} \sigma_s^4 \rho_{ssss}^2 \\
 & + O\left(\|\boldsymbol{\sigma}\|_\infty^5\right), \tag{43}
 \end{aligned}$$

$$\begin{aligned}
 \mathbf{U}(-\mathbf{b}_s) & = \mathbf{U}_0 - \mathbf{U}_s^I \sigma_s \rho_s^{\frac{1}{2}} + \mathbf{U}_{ss}^{\text{II}} \sigma_s^2 \rho_{ssss} \\
 & - \mathbf{U}_{sss}^{\text{III}} \sigma_s^3 \rho_{ssss}^{\frac{3}{2}} + \mathbf{U}_{ssss}^{IV} \sigma_s^4 \rho_{ssss}^2
 \end{aligned}$$

$$+ O\left(\|\boldsymbol{\sigma}\|_\infty^5\right). \tag{44}$$

By adding Eqs. (43) and (44), and subtracting Eq. (44) from Eq. (43), the following equations can be obtained

$$\frac{\mathbf{z}_s}{2\rho_{ssss}} + O\left(\|\boldsymbol{\sigma}\|_\infty^6\right) = \mathbf{U}_{ss}^{\text{II}} \sigma_s^2 + \mathbf{U}_{ssss}^{IV} \rho_{ssss} \sigma_s^4, \tag{45}$$

$$\frac{\mathbf{w}_s}{2\sqrt{\rho_{ssss}}} + O\left(\|\boldsymbol{\sigma}\|_\infty^5\right) = \mathbf{U}_s^I \sigma_s + \mathbf{U}_{sss}^{\text{III}} \rho_{ssss} \sigma_s^3, \tag{46}$$

noting that

$$\mathbf{z}_s = \mathbf{U}(\mathbf{b}_s) + \mathbf{U}(-\mathbf{b}_s) - 2\mathbf{U}_0, \tag{47}$$

$$\mathbf{w}_s = \mathbf{U}(\mathbf{b}_s) - \mathbf{U}(-\mathbf{b}_s). \tag{48}$$

Through Eqs. (45) and (46), we have

$$\left( \frac{\mathbf{z}_s}{2\rho_{ssss}} \right) \left( \frac{\mathbf{z}_s}{2\rho_{ssss}} \right)^T = \mathbf{U}_{ss}^{\text{II}} \mathbf{U}_{ss}^{\text{II}T} \sigma_s^4 + O\left(\|\boldsymbol{\sigma}\|_\infty^6\right), \tag{49}$$

$$\begin{aligned}
 \left( \frac{\mathbf{w}_s}{2\sqrt{\rho_{ssss}}} \right) \left( \frac{\mathbf{w}_s}{2\sqrt{\rho_{ssss}}} \right)^T & = \mathbf{U}_s^I \mathbf{U}_s^{IT} \sigma_s^2 \\
 & + \mathbf{U}_s^I \mathbf{U}_{sss}^{\text{III}T} \sigma_s^4 \rho_{ssss} + \mathbf{U}_{sss}^{\text{III}} \mathbf{U}_s^{IT} \sigma_s^4 \rho_{ssss} \\
 & + O\left(\|\boldsymbol{\sigma}\|_\infty^4\right). \tag{50}
 \end{aligned}$$

Substituting Eqs. (49) and (50) into Eqs. (39) and (40), we have

$$\mathbf{E}(\mathbf{U}(\boldsymbol{\alpha})) = \mathbf{U}_0 + \frac{1}{2} \sum_{s=1}^q \frac{\mathbf{z}_s}{\rho_{ssss}} + O\left(\|\boldsymbol{\sigma}\|_\infty^4\right), \tag{51}$$

$$\begin{aligned}
 \text{Cov}(\mathbf{U}(\boldsymbol{\alpha}), \mathbf{U}(\boldsymbol{\alpha})) & = \frac{1}{4} \sum_{s=1}^q \left[ \frac{\mathbf{w}_s \mathbf{w}_s^T}{\rho_{ssss}} + \frac{\mathbf{z}_s \mathbf{z}_s^T}{\rho_{ssss}^2} (\rho_{ssss} - 1) \right] \\
 & + O\left(\|\boldsymbol{\sigma}\|_\infty^4\right). \tag{52}
 \end{aligned}$$

$\mathbf{U}(\pm \mathbf{b}_s)$  can be obtained easily by solving the governing equation with  $\pm \mathbf{b}_s$

$$\mathbf{K}(\pm \mathbf{b}_s) \mathbf{U}(\pm \mathbf{b}_s) = \mathbf{F}. \tag{53}$$

Similarly, Eqs. (51) and (52) contain some higher-order terms that do not exist in Eqs. (33) and (35), which leads to a further improvement in accuracy.

For the coefficients  $\rho_{sss}$  and  $\rho_{ssss}$ , the moment generating function  $M_\alpha(t)$  defined by Eq. (54) is introduced to calculate the mean  $\mathbf{E}(\sigma_s \sigma_s \sigma_s)$  and  $\mathbf{E}(\sigma_s \sigma_s \sigma_s \sigma_s)$ .

$$M_\alpha(t) = \mathbf{E}(e^{t\boldsymbol{\alpha}}). \tag{54}$$

If the random variable  $\alpha$  is Gaussian,  $M_\alpha(t)$  can be written as

$$M_\alpha(t) = e^{t\mu + \frac{t^2\sigma^2}{2}}. \tag{55}$$

Due to the random variables obtained by K–L expansion being standard Gaussian with zero mean and unit variance, Eq. (55) can be rewritten as

$$M_\alpha(t) = e^{\frac{t^2}{2}}, \tag{56}$$

there,  $E(\sigma_s\sigma_s\sigma_s)$  and  $E(\sigma_s\sigma_s\sigma_s\sigma_s)$  can be calculated by the following equations.

$$\begin{aligned} E(\sigma_s\sigma_s\sigma_s) &= \left. \frac{d^3 M_\alpha(t)}{dt^3} \right|_{t=0} \\ &= \left( 3e^{\frac{t^2}{2}}t + e^{\frac{t^2}{2}}t^3 \right) \Big|_{t=0} = 0, \end{aligned} \tag{57}$$

$$\begin{aligned} E(\sigma_s\sigma_s\sigma_s\sigma_s) &= \left. \frac{d^4 M_\alpha(t)}{dt^4} \right|_{t=0} \\ &= \left( 3e^{\frac{t^2}{2}} + 6e^{\frac{t^2}{2}}t^2 + e^{\frac{t^2}{2}}t^4 \right) \Big|_{t=0} = 3. \end{aligned} \tag{58}$$

Hence, for the Gaussian random field,  $\rho_{SS} = 0$  and  $\rho_{SSSS} = 3$ ; Eqs. (23) and (42) can be rewritten as

$$\mathbf{a}_s = \left( \underbrace{0, \dots, 0}_{s-1}, 1, \underbrace{0, \dots, 0}_{q-s} \right), \tag{59}$$

$$\mathbf{b}_s = \left( \underbrace{0, \dots, 0}_{s-1}, \sqrt{3}, \underbrace{0, \dots, 0}_{q-s} \right). \tag{60}$$

From the equations in this section, the procedures of calculation of MPSFEM include  $2q + 1$  calculations, which is the same as PSFEM, but does not require taking the partial derivatives of the system matrix with respect to  $\alpha$  and is more accurate than PSFEM. Meanwhile, compared to polynomial chaos expansion techniques, MPSFEM can directly utilize the original computational scheme of finite element method; and compared to non-invasive techniques, MPSFEM is relatively less computationally intensive. Therefore, MPSFEM is relatively suitable for static stochastic analysis.

### 4 JC method

JC method [44] that has been recommended by the Joint Committee on Structural Safety (JCSS) is introduced in combination with MPSFEM to calculate structural reliability.

The first step is to assume the checking points, i.e., to assume a set of values of  $\alpha^*$ , usually taking  $\alpha_i^* = \mu_{\alpha_i}$ , where

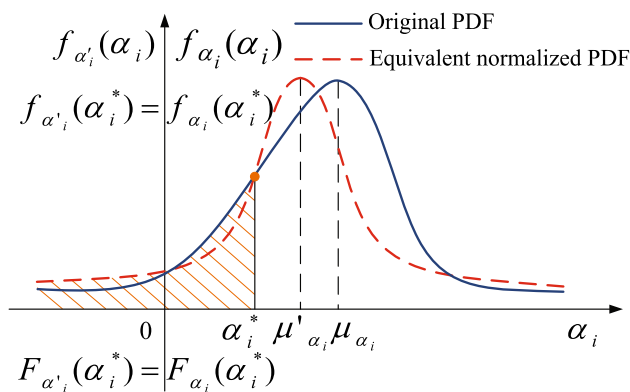


Fig. 1 Equivalent normalization for the non-normally distributed random variable

$\alpha_i^*$  is a checking point and  $\mu_{\alpha_i}$  is the mean of the random variable  $\alpha_i$ .

Then the non-normally distributed random variables need to be normalized; the conditions are as follows.

$$F_{\alpha'_i}(\alpha_i^*) = F_{\alpha_i}(\alpha_i^*) = \Phi \left( \frac{\alpha_i^* - \mu_{\alpha'_i}}{\sigma_{\alpha'_i}} \right), \tag{61}$$

$$f_{\alpha'_i}(\alpha_i^*) = f_{\alpha_i}(\alpha_i^*) = \frac{1}{\sigma_{\alpha'_i}} \phi \left( \frac{\alpha_i^* - \mu_{\alpha'_i}}{\sigma_{\alpha'_i}} \right), \tag{62}$$

where  $F_{\alpha_i}(\bullet)$  and  $F_{\alpha'_i}(\bullet)$  are the cumulative distribution functions (CDF) of the random variable  $\alpha_i$  and equivalent normalized random variable  $\alpha'_i$ , respectively;  $f_{\alpha_i}(\bullet)$  and  $f_{\alpha'_i}(\bullet)$  are the probability density functions (PDF) of the random variable  $\alpha_i$  and equivalent normalized random variable  $\alpha'_i$ , respectively;  $\mu_{\alpha'_i}$  and  $\sigma_{\alpha'_i}$  are the mean and standard deviation of  $\alpha'_i$ , respectively;  $\Phi(\bullet)$  and  $\phi(\bullet)$  are the CDF and PDF of the standard normally distributed random variable, respectively.

As shown in Fig. 1, Eqs. (61) and (62) mean that the values of the CDFs are equal and the values of the PDFs are equal at the checking point.

The derivations of Eqs. (61) and (62) yields

$$\mu_{\alpha'_i} = \alpha_i^* - \Phi^{-1} (F_{\alpha_i}(\alpha_i^*)) \sigma_{\alpha_i}, \tag{63}$$

$$\sigma_{\alpha'_i} = \frac{\phi (\Phi^{-1} (F_{\alpha_i}(\alpha_i^*)))}{f_{\alpha_i}(\alpha_i^*)}, \tag{64}$$

therefore, if the random variable is non-normally distributed,  $\mu_{\alpha_i}$  and  $\sigma_{\alpha_i}$  need to be replaced by  $\mu_{\alpha'_i}$  and  $\sigma_{\alpha'_i}$  in the following equations in this section.

After normalizing the random variables, it is assumed that the random variables are independent. If they are not, they should be transformed into independent random variables by orthogonal transformation. Then the first order Taylor expansion

sion of the performance function of structure  $g(\alpha)$  at the checking points  $\alpha^*$  can be expressed as

$$Z = g(\alpha^*) + \sum_{i=1}^q \left. \frac{\partial g}{\partial \alpha_i} \right|_{\alpha^*} (\alpha_i - \alpha_i^*), \tag{65}$$

hence the mean and standard deviation of  $Z$  can be written as

$$\mu_Z = g(\alpha^*) + \sum_{i=1}^q \left. \frac{\partial g}{\partial \alpha_i} \right|_{\alpha^*} (\mu_{\alpha_i} - \alpha_i^*), \tag{66}$$

$$\sigma_Z = \sqrt{\sum_{i=1}^q \left( \left. \frac{\partial g}{\partial \alpha_i} \right|_{\alpha^*} \sigma_{\alpha_i} \right)^2}. \tag{67}$$

By definition, the reliability index can be written as

$$\beta = \frac{\mu_Z}{\sigma_Z} = \frac{g(\alpha^*) + \sum_{i=1}^q \left. \frac{\partial g}{\partial \alpha_i} \right|_{\alpha^*} (\mu_{\alpha_i} - \alpha_i^*)}{\sqrt{\sum_{i=1}^q \left( \left. \frac{\partial g}{\partial \alpha_i} \right|_{\alpha^*} \sigma_{\alpha_i} \right)^2}}. \tag{68}$$

When the structure is in the limit state, the limit state function is

$$Z = g(\alpha^*) = 0, \tag{69}$$

then Eq. (68) can be rewritten as

$$\beta = \frac{\mu_Z}{\sigma_Z} = \frac{\sum_{i=1}^q \left. \frac{\partial g}{\partial \alpha_i} \right|_{\alpha^*} (\mu_{\alpha_i} - \alpha_i^*)}{\sqrt{\sum_{i=1}^q \left( \left. \frac{\partial g}{\partial \alpha_i} \right|_{\alpha^*} \sigma_{\alpha_i} \right)^2}}. \tag{70}$$

The iterative equation for the checking point is as follows.

$$\alpha_i^* = \mu_{\alpha_i} + \beta \phi_i \sigma_{\alpha_i}, \tag{71}$$

where  $\phi_i$  is the sensitivity coefficient, which is defined by

$$\phi_i = \frac{- \left. \frac{\partial g}{\partial \alpha_i} \right|_{\alpha^*} \sigma_{\alpha_i}}{\sqrt{\sum_{i=1}^q \left( \left. \frac{\partial g}{\partial \alpha_i} \right|_{\alpha^*} \sigma_{\alpha_i} \right)^2}}. \tag{72}$$

The calculation steps of JC method can be organized as follows:

- (1) Set the initial checking points  $\alpha^*$ .
- (2) Equivalent normalizing the non-normally distributed random vector at  $\alpha^*$ .
- (3) Calculating the sensitivity coefficient  $\phi_i$  by Eq. (72).
- (4) Calculating the reliability index  $\beta$  by Eq. (70).
- (5) Calculating the new checking points by Eq. (71).

- (6) Substituting the new checking points into steps (2) to (5) and the calculation is repeated until  $\beta$  obtained from the two calculations is less than the specified value, then  $\beta$  obtained from the last iteration is the reliability index.

The failure probability  $p_f$  can be written as

$$p_f = 1 - \phi(\beta) = \phi(-\beta). \tag{73}$$

## 5 The promotions of KL-MPSM

Based on the theories in the above sections, we promote MPSFEM to the static stochastic analysis for the plane problem and plane frame structure, corresponding to two-dimensional random fields and one-dimensional random fields, respectively. In static stochastic computation, KL-MPSM can obtain the mean and variance of the displacement of the critical node. In the reliability analysis, KL-MPSM can provide failure probability for structural reliability evaluations by combining with JC method.

### 5.1 Static stochastic analysis for plane problems

Many engineering structures are reduced to plane problems (plane stress problems and plane strain problems) in computation, such as deep beams, slabs, etc. In this subsection, the computational scheme of KL-MPSM for the static stochastic analysis of plane problems is described in detail by regarding Poisson’s ratio as a Gaussian random field.

For plane problems, we adopt isoparametric element with four nodes. The elastic matrix  $D$  can be expressed as

$$D = \frac{E}{1 - \nu^2} \begin{bmatrix} 1 & \nu & 0 \\ \nu & 1 & 0 \\ 0 & 0 & \frac{1-\nu}{2} \end{bmatrix}, \tag{74}$$

where  $E$  is Young’s modulus and  $\nu$  is Poisson’s ratio.

In PSFEM, the partial derivatives of the stiffness matrix with respect to random variables are required. If Poisson’s ratio  $\nu$  is regarded as a random field, the computation procedures of taking the partial derivatives will involve complex character operations, and the programming efficiency will be significantly reduced; therefore, for the problems like this, PSFEM is challenging to deal with; however, in KL-MPSM, the elastic matrix  $D(\pm b_i)$ , in which the random vector has been replaced with the deterministic vector, can be written as

$$D(\pm b_i) = \frac{E}{1 - \nu^{*2}} \begin{bmatrix} 1 & \nu^* & 0 \\ \nu^* & 1 & 0 \\ 0 & 0 & \frac{1-\nu^*}{2} \end{bmatrix}, \tag{75}$$



where  $v^* = \bar{v} \pm \sqrt{3\lambda_i} f_i(x, y)$ .

Then the element stiffness matrix  $K^e(\pm b_i)$  of KL-MPSM in plane problem can be obtained by the integral of the isoparametric element, which can be expressed as

$$K^e(\pm b_i) = \int_{-1}^1 \int_{-1}^1 \mathbf{B}^T \mathbf{D}(\pm b_i) \mathbf{B} t |J| d\alpha d\beta, \tag{76}$$

where  $\mathbf{B}$  is strain transformation matrix;  $t$  denotes thickness;  $J$  expresses Jacobian matrix.

When Young’s modulus  $E$  is regarded as a random field, the element stiffness matrix can be obtained similarly. Then  $K^e(\pm b_i)$  is assembled to obtain the global stiffness matrix  $\mathbf{K}(\pm b_i)$ , and MPSFEM can get the second-order estimates of the structural response.

For reliability analysis, considering the random variables input by K–L expansion, the performance function of the structure can be written as

$$Z = g(\boldsymbol{\xi}(\theta)). \tag{77}$$

From Eqs. (70) and (72), we can see that the most critical parameter is the partial derivative of the performance function with respect to the random variables at the checking points, which can be written as  $\frac{\partial g}{\partial \xi_i(\theta)} \Big|_{\boldsymbol{\xi}^*(\theta)}$ . Equation (77) is usually implicit, which means that  $\xi_i(\theta)$  does not usually appear in Eq. (77), and the distribution of the structural response random variable is often unknown. These make it difficult to conduct equivalent normalization and solve Eqs. (70) and (72). Therefore, an intermediate structural response  $U$ , since performance functions are generally related to structural responses, is introduced. The equation of calculating the partial derivative can be expanded as

$$\frac{\partial g}{\partial \xi_i(\theta)} = \frac{\partial g}{\partial U} \frac{\partial U}{\partial \xi_i(\theta)}. \tag{78}$$

In this subsection, we use the displacement of the key node to control the structural failure mode; hence,  $U$  is the displacement of the control node. Then we assume the following equation.

$$\frac{\partial U}{\partial \xi_i(\theta)} = U_i^I, \tag{79}$$

where  $U_i^I$  is the element corresponding to the control node in the vector  $\mathbf{U}_i^I$ , and its value is independent of the value of  $\xi_i(\theta)$  [45]. In fact,  $U_i^I$  can also be interpreted as the first-order sensitivity of the intermediate response to the random variable  $\xi_i(\theta)$ .

In PSFEM,  $U_i^I$  can be calculated by Eq. (12) with the partial derivative of stiffness matrix with respect to random variable  $\xi_i(\theta)$ . The difficulties have already been discussed in the previous sections. Whereas in MPSFEM,  $U_i^I$  can be

obtained by adding and subtracting the Eqs. (24) and (25) easily, i.e., Eqs. (27) and (29). Since the mean of  $\xi_i(\theta)$  is 0 and standard deviation is 1, Eq. (27) can be rewritten as

$$U_i^I = \frac{w_i}{2} + (\|\sigma\|_\infty^3). \tag{80}$$

After that,  $U_i^I$  can be determined according to the control node from  $\mathbf{U}_i^I$ . Hence, we have

$$\frac{\partial g}{\partial \xi_i(\theta)} \Big|_{\boldsymbol{\xi}^*(\theta)} = \frac{\partial g}{\partial U} \Big|_{\boldsymbol{\xi}^*(\theta)} U_i^I. \tag{81}$$

The Eqs. (72), (70), and (71) can be rewritten as

$$\phi_i = \frac{-\frac{\partial g}{\partial U} \Big|_{\boldsymbol{\xi}^*(\theta)} U_i^I}{\sqrt{\sum_{i=1}^n \left( \frac{\partial g}{\partial U} \Big|_{\boldsymbol{\xi}^*(\theta)} U_i^I \right)^2}}, \tag{82}$$

$$\beta = \frac{g(\boldsymbol{\xi}^*(\theta)) - \sum_{i=1}^n \frac{\partial g}{\partial U} \Big|_{\boldsymbol{\xi}^*(\theta)} U_i^I \xi_i^*(\theta)}{\sqrt{\sum_{i=1}^n \left( \frac{\partial g}{\partial U} \Big|_{\boldsymbol{\xi}^*(\theta)} U_i^I \right)^2}}, \tag{83}$$

$$\xi_i^*(\theta) = \beta \phi_i. \tag{84}$$

Then we can get the reliability index and failure probability of the structure by the iterative computations of Eqs. (82), (83), and (84).

### 5.2 Static stochastic analysis for plane frame structures

In the static stochastic computation for plane frame structures, beams and columns are uniformly regarded as one-dimensional beam elements. The computation procedures are the same as plane problems, so they will not be repeated here.

In the reliability analysis for plane frame structures, the simplest performance function can be written as

$$Z = R - S, \tag{85}$$

where  $R$  denotes structural resistance, and  $S$  denotes action effect. When the external load does not change with time, the ultimate load  $P_u$  is the structural resistance.

In Ref. [35], Wu argued that MPSFEM could solve other problems with the same computation scheme, and the problems hold the same governing equations form. The form of the governing equations can be expressed as

$$L(\mathbf{P}_u(\boldsymbol{\xi}(\theta)), \boldsymbol{\xi}(\theta)) = 0. \tag{86}$$

The stochastic ultimate load  $P_u(\xi(\theta))$  can be expanded as

$$\begin{aligned}
 P_u(\xi(\theta)) &= P_{u0} + \sum_{i=1}^q P_{ui}^I \xi_i(\theta) \\
 &+ \sum_{i=1}^q \sum_{j=i}^q P_{uij}^{II} \xi_i(\theta) \xi_j(\theta) \\
 &+ \sum_{i=1}^q \sum_{j=i}^q \sum_{k=j}^q P_{uijk}^{III} \xi_i(\theta) \xi_j(\theta) \xi_k(\theta) \\
 &+ \sum_{i=1}^q \sum_{j=i}^q \sum_{k=j}^q \sum_{l=k}^q P_{uijkl}^{IV} \xi_i(\theta) \xi_j(\theta) \xi_k(\theta) \xi_l(\theta) \\
 &+ \left( \|\xi\|_\infty^5 \right). \tag{87}
 \end{aligned}$$

Using the same method referred in the Sect. 3.2, we have

$$E(P_u(\xi(\theta))) = P_{u0} + \frac{1}{2} \sum_{i=1}^q \frac{z_i}{\rho_{iiii}} + O(\|\sigma\|_\infty^4), \tag{88}$$

$$\begin{aligned}
 &\text{Cov}(P_u(\xi(\theta)), P_u(\xi(\theta))) \\
 &= \frac{1}{4} \sum_{i=1}^q \left[ \frac{w_i w_i^T}{\rho_{iiii}} + \frac{z_i z_i^T}{\rho_{iiii}^2} (\rho_{iiii} - 1) \right] + O(\|\sigma\|_\infty^4). \tag{89}
 \end{aligned}$$

where

$$z_i = P_u(b_i) + P_u(-b_i) - 2P_u(b_0). \tag{90}$$

$$w_i = P_u(b_i) - P_u(-b_i). \tag{91}$$

In Sect. 5.1, we have discussed how to apply JC method for reliability analysis when the distribution of the structural response random variable is unknown. In this subsection, we use the ultimate load to control the failure mode. In engineering, in terms of the central limit theorem, no matter what distribution the random variables obey, the ultimate load can be approximately considered to obey lognormal distribution. After obtaining the second-order estimates, PDF, and CDF of  $P_u(\xi(\theta))$ , the equivalent normalization is conducted to transform  $P_u(\xi(\theta))$  into normal distribution, and then iterative calculations of Eqs. (72), (70), and (71) can be performed to obtain the reliability index.  $P_u(\pm b_i)$  in the above equations can be obtained by the elastic-plastic incremental method (step-by-step method) [46].

In the computations of elastic-plastic incremental method, the following basic assumptions should be followed:

- (1) When a plastic hinge appears in the structure, the plastic zone degenerates into a section, and the rest are still elastic zones.

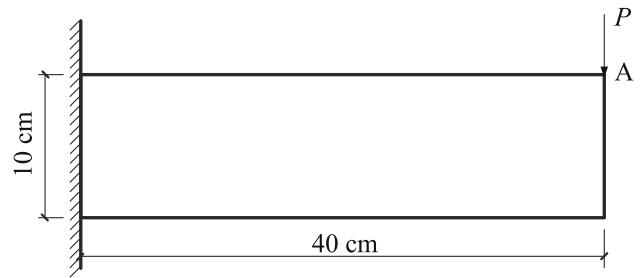


Fig. 2 The geometry of the cantilever deep beam

- (2) The external loads need to be converted into node loads and act on the structure step by step in proportion; plastic hinges only appear at the nodes.
- (3) The ultimate moments of each bar are constants, and ultimate moments of different bars can be different.
- (4) Axial and shear forces do not affect the ultimate moments.
- (5) The material of all bars is ideal elastic-plastic.

## 6 Numerical examples

In this section, we compare the KL-MPSM with Monte Carlo finite element method and perturbation stochastic finite element method (in the following figures, we use MCM and PSM to represent them). The computation procedures of MCM and PSM can be deduced based on the same idea of KL-MPSM, and the progress will not be repeated here. The results obtained by MCM are treated as the standard value.

### 6.1 The deep beam with a two-dimensional random field

In engineering, deep beams are often simplified as plane problems for analysis. Figure 2 shows a cantilever deep beam with a two-dimensional (2D) random field, and its structural parameters are as follows.

The horizontal length is 40 cm, the vertical length is 10 cm, the left end is fixed, and the other three ends are free. The vertical concentrated force  $P$  acts on point A, and  $P = 1000$  N. Young’s modulus of the material  $E = 3 \times 10^7$  N/cm<sup>2</sup>. Set the thickness  $t$  to 1 cm. Poisson’s ratio  $\nu$  is assumed to be a two-dimensional stationary Gaussian random field, and its mean value  $\bar{\nu} = 0.3$ . The horizontal relative length  $c_x = 40$  cm, the vertical relative length  $c_y = 5$  cm. The type of covariance function is Gaussian, and it can be written as

$$C(x_1, x_2; y_1, y_2) = \sigma^2 e^{-(x_1-x_2)^2/c_x^2 - (y_1-y_2)^2/c_y^2}.$$

The two-dimensional random field shown in Fig. 2 can be discretized in two directions, and the results are combined to

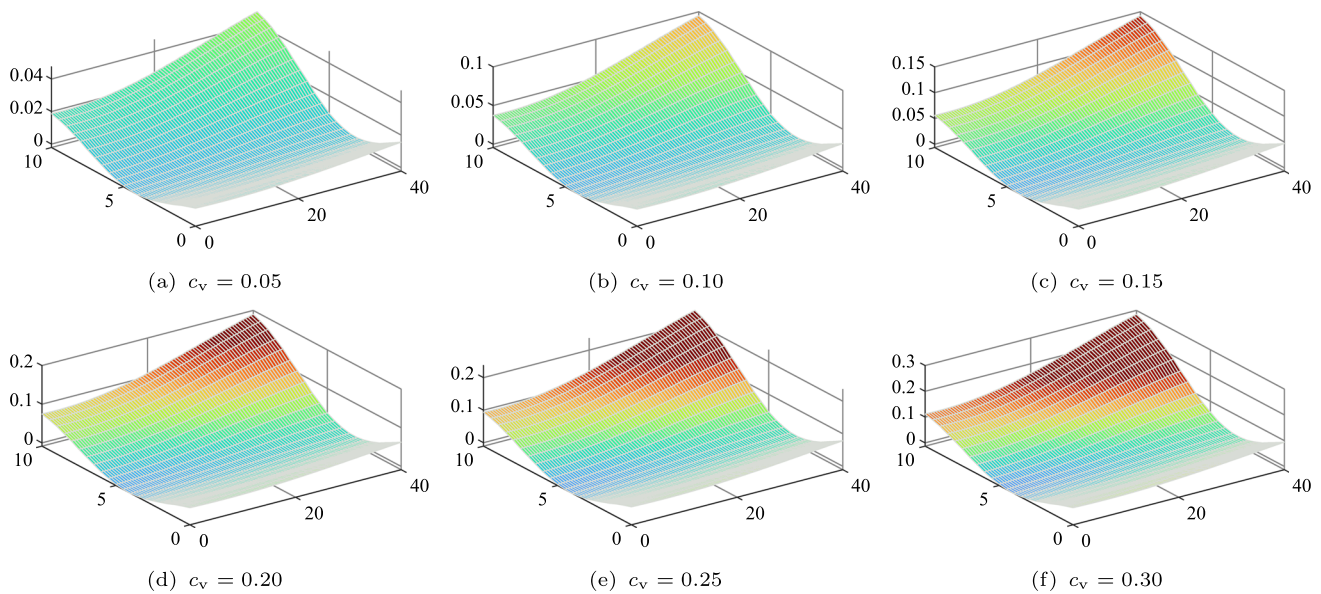


**Fig. 3** Superposition of the first five order eigenvalues and eigenfunctions  $\sqrt{\lambda_i} f_i(x)$  with different coefficients of variation  $c_v$

obtain the global discretization consequence. Please refer to Ref. [23] for the exact procedures.

Firstly, the random field is discretized by K–L method, and the first five terms of eigenvalues and eigenfunctions are truncated. The Simulation results under different coefficients of variation ( $c_v$ ) are shown in Fig. 3. In Fig. 3, we assume that the random variable vector  $\xi(\theta)$  is a unit vector and plot the function graphs of  $\sqrt{\lambda_i} f_i(x)$  by Matlab. It can be observed that the variation degree of the random field increases significantly with the increase of coefficient of variation  $c_v$ . In terms of the previous research, the accuracy of PSFEM will rapidly decrease after  $c_v$  reaches 0.15. Therefore, this paper chooses to compare KL-MPSM with other methods within the range of  $c_v$  0.05 to 0.25. The deep beam is discretized into four elements uniformly in the horizontal direction, and the element adopts isoparametric element with four nodes.

In order to obtain accurate data, Latin hypercube sampling method [47] is used in MCM to draw 20000 samples, and the simulation results obtained by different methods with different  $c_v$  are shown in Fig. 4. Figure 4 shows that the results of KL-MPSM and MCM are very close in the range of  $c_v$  0 to 0.15, and KL-MPSM also maintains good accuracy in the range of  $c_v$  0.15 to 0.25. In this numerical example, PSM is not used for the reason that the Poisson’s ratio is regarded as a random field, and the calculations of taking partial derivatives involve many character operations, which will significantly increase the difficulty of programming; at the same time, the efficiency advantages of KL-MPSM will not be reflected intuitively, so there is of little significance to use PSM. Compared with PSM, KL-MPSM only needs

to replace the random vector with deterministic vectors, and there is no need to take the partial derivatives of the stiffness matrix. Hence the steps of KL-MPSM are straightforward and save a lot of programming time.

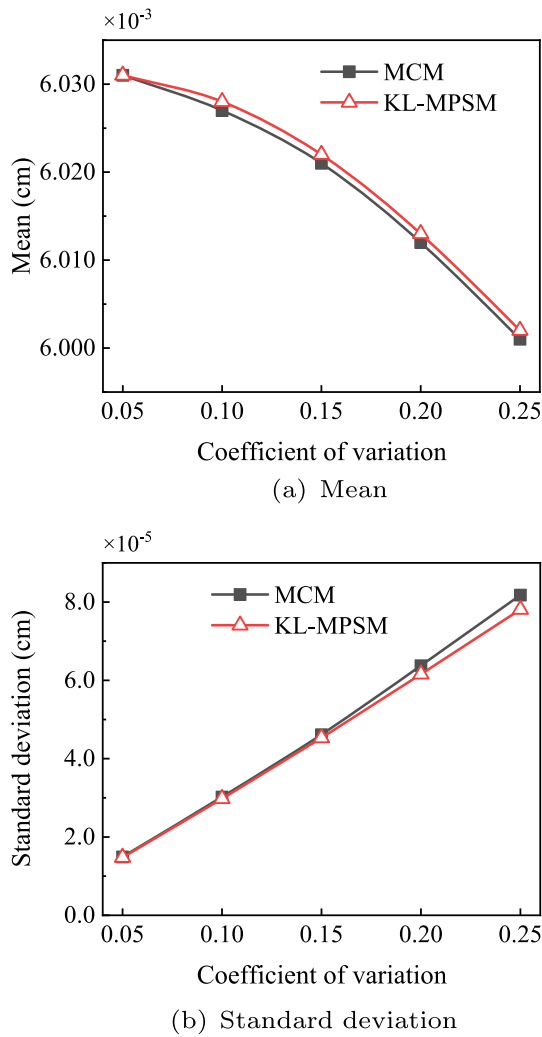
In the same structure, regarding Young’s modulus as a Gaussian random field, its mean  $E = 3 \times 10^7$  N/cm<sup>2</sup>, and Poisson’s ratio  $\nu = 0.3$ . The other parameters remain unchanged. The vertical displacement of point A controls the failure mode, and the performance function is nonlinear, which can be written as

$$Z = 0.007^2 - (u_A - \bar{u}_A)^2,$$

where  $u_A$  is the vertical displacement at point A, and  $\bar{u}_A$  is the mean of  $u_A$ .

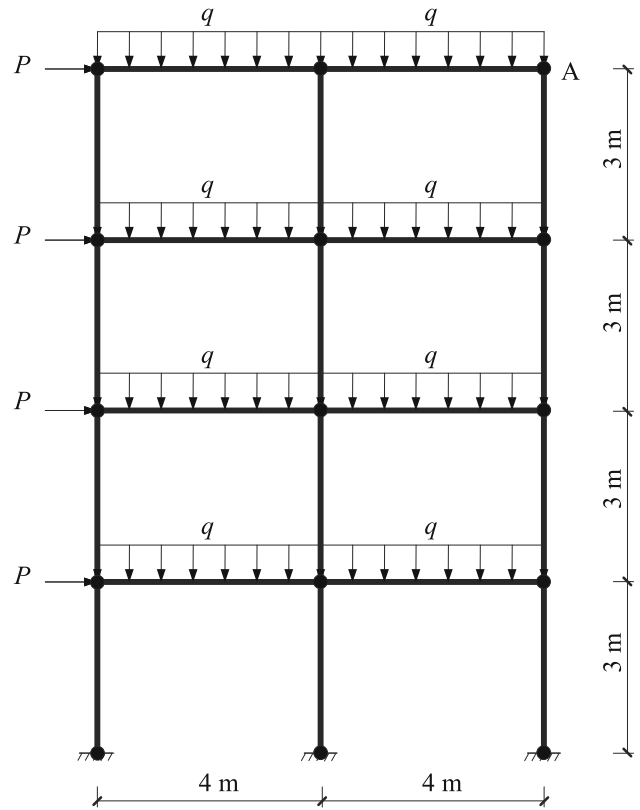
In this numerical example, we use the approach for reliability analysis proposed in 5.1. Therefore,  $u_A$  is the intermediate structural response. The value of  $U_1^I$ ,  $U_2^I$ , and  $U_3^I$  are listed in Tab. 1. It can be seen that when  $c_v$  is in the range of 0~0.15, the difference in accuracy between the two methods is not large; when  $c_v$  is larger than 0.15, the difference is gradually obvious. This is because Eq. (80) contains some higher-order terms that Eq. (12) does not, with higher accuracy.

Table 2 shows that the results of the three methods are close in the range of  $c_v$  0–0.15; when  $c_v$  is greater than 0.15, the accuracy of KL-MPSM and PSM begins to decrease, and the accuracy of KL-MPSM is slightly greater than that of PSM. These results are consistent with the discussion for Table 1.



**Fig. 4** Mean and standard deviation of the vertical displacement at point A calculated by MCM and KL-MPSM with different coefficients of variation  $c_v$

In summary, KL-MPSM is an effective tool for static stochastic analysis of plane problems in the case of low-level uncertainties ( $c_v$  less than 0.15). When the requirement of accuracy is not strict, it is also suitable in the case of  $c_v$  greater than 0.15.



**Fig. 5** The geometry of the plane multilayer frame

### 6.2 The plane frame with one-dimensional random fields

Figure 5 shows a plane multilayer frame with one-dimensional random fields, and its structural parameters are as follows.

The span is 4 m; the story height is 3 m; the section area of columns  $A_c = 0.35 \times 0.35 \text{ m}^2$ , and the moment of inertia  $I_c = 1.25 \times 10^{-3} \text{ m}^4$ ; the section area of beams  $A_b = 0.35 \times 0.6 \text{ m}^2$ , and the moment of inertia  $I_b = 6.3 \times 10^{-3} \text{ m}^4$ ; concentrated forces  $P = 20 \text{ KN}$  act on vertexes of left columns. The uniform load  $q$  acts on each beam, and  $q = 100 \text{ KN/m}$ . Young’s modulus of the material is regarded as a Gaussian random field on each component.

**Table 1** The first-order sensitivity of the intermediate response  $U$  to the random variable  $\xi_1(\theta)$ ,  $\xi_2(\theta)$ , and  $\xi_3(\theta)$  calculated by KL-MPSM and PSM with different coefficients of variation  $c_v$

$c_v$	KL-MPSM			PSM		
	$U_1^1(\times 10^{-4})$	$U_2^1(\times 10^{-6})$	$U_3^1(\times 10^{-4})$	$U_1^1(\times 10^{-4})$	$U_2^1(\times 10^{-6})$	$U_3^1(\times 10^{-4})$
0.05	-1.982	0.865	0.625	-1.983	0.864	0.625
0.10	-3.978	1.733	1.252	-3.961	1.728	1.250
0.15	-6.000	-2.607	-1.880	-5.941	-2.593	-1.875
0.20	-8.062	3.490	2.511	-7.921	3.457	2.500
0.25	-10.179	-4.387	3.146	-9.901	-4.321	3.126

**Table 2** The reliability index and failure probability of the deep beam calculated by MCM, KL-MPSM, and PSM with different coefficients of variation  $c_v$

$c_v$	MCM		KL-MPSM		PSM	
	Reliability index	Failure probability (%)	Reliability index	Failure probability (%)	Reliability index	Failure probability (%)
0.05	2.929	0.170	2.935	0.167	2.935	0.167
0.10	1.249	10.59	1.256	10.456	1.256	10.455
0.15	0.553	29.00	0.564	28.630	0.564	28.62
0.20	0.141	44.395	0.155	43.826	0.157	43.781
0.25	-0.164	56.524	-0.132	55.232	-0.129	55.129

**Table 3** The parameters of the column and beam random fields in the static stochastic computation

Parameters	Column	Beam
Covariance function	Exponential	Gaussian
Mean value(N/m <sup>2</sup> )	$2.1 \times 10^{11}$	$2.1 \times 10^{11}$
Relative length (m)	1	2
K–L terms	13	3
Wavelet coefficient	9	9

The beams and columns work in different conditions, and various external factors influence them; therefore, the random fields are independent. The parameters of the random fields are shown in Table 3.

In this kind of problem with multiple independent random fields, the random fields should be discretized independently; after that, the random variables obtained are combined into a random vector, then substituting the random vector into MPSFEM and JC method. The plane multilayer frame contains 20 independent random fields, and 180 random variables are obtained according to the K–L terms. The random variables can be divided into

$$\begin{aligned} \xi_1^C(\theta) &= \{\xi_1(\theta), \dots, \xi_{13}(\theta)\}, \\ &\dots, \\ \xi_{12}^C(\theta) &= \{\xi_{144}(\theta), \dots, \xi_{156}(\theta)\}, \\ \xi_1^B(\theta) &= \{\xi_{157}(\theta), \xi_{158}(\theta), \xi_{159}(\theta)\}, \\ &\dots, \\ \xi_8^B(\theta) &= \{\xi_{178}(\theta), \xi_{179}(\theta), \xi_{180}(\theta)\}, \end{aligned}$$

where  $\xi_i^C(\theta)$  and  $\xi_i^B(\theta)$  denote the random vectors of column and beam random fields, respectively.

Combining these random vectors together to obtain

$$\begin{aligned} \xi(\theta) &= \{\xi_1^C(\theta), \dots, \xi_{12}^C(\theta), \xi_1^B(\theta), \dots, \xi_8^B(\theta)\} \\ &= \{\xi_1(\theta), \xi_2(\theta), \dots, \xi_{180}(\theta)\}, \end{aligned} \tag{92}$$

and then substituting  $\xi(\theta)$  into MPSFEM and JC method.

Since the random fields are independent,  $c_v$  can also be different. However, in this example, in order to compare the results conveniently,  $c_v$  of each random field is the same. Latin hypercube sampling method is used in MCM to draw 20,000 samples. The mean and standard deviation of the horizontal displacement at point A are shown in Fig. 6.

Figure 6 shows that the application range and accuracy superiority of KL-MPSM is consistent with the example of the deep beam, and the feasibility of KL-MPSM is further verified. From the results, KL-MPSM still maintains good accuracy in the case that random fields hold different types of covariance functions, while the accuracy of PSM shows a sig-

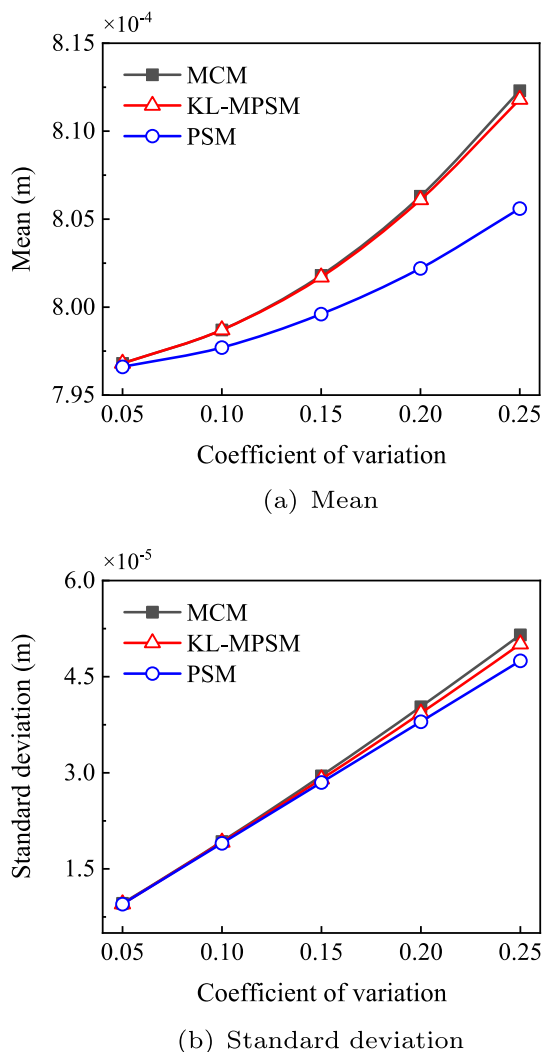


**Fig. 6** Mean and standard deviation of the horizontal displacement at point A calculated by MCM, KL-MPSM, and PSM with different coefficients of variation  $c_v$

nificant decrease. Therefore, this numerical example proves that KL-MPSM has good accuracy and applicability in the static stochastic computation for plane frame structures.

Next, introduce the yield strength of the material to compute the ultimate load  $P_u$  of the structure, and then the reliability analysis is conducted. The yield strength is treated as Gaussian random fields; the parameters of the random fields are shown in Table 4. Young’s modulus  $E = 2 \times 10^{11}$  N/m<sup>2</sup>, the other structural parameters remain unchanged. In order to demonstrate the feasibility of KL-MPSM for reliability analyses of plane frames, the reliability index and failure probability are computed by MCM and KL-MPSM, respectively. For KL-MPSM, since the distribution of the responses is known, we use the method proposed in Sect. 5.2. The performance function can be written as

$$Z = R - 1550000.$$

**Table 4** The parameters of the column and beam random fields in the reliability analysis

Parameters	Column	Beam
Covariance function	Gaussian	Gaussian
Mean value (Pa)	$3 \times 10^8$	$3 \times 10^8$
Relative length (m)	1	2
K–L terms	3	3
Wavelet coefficient	9	9

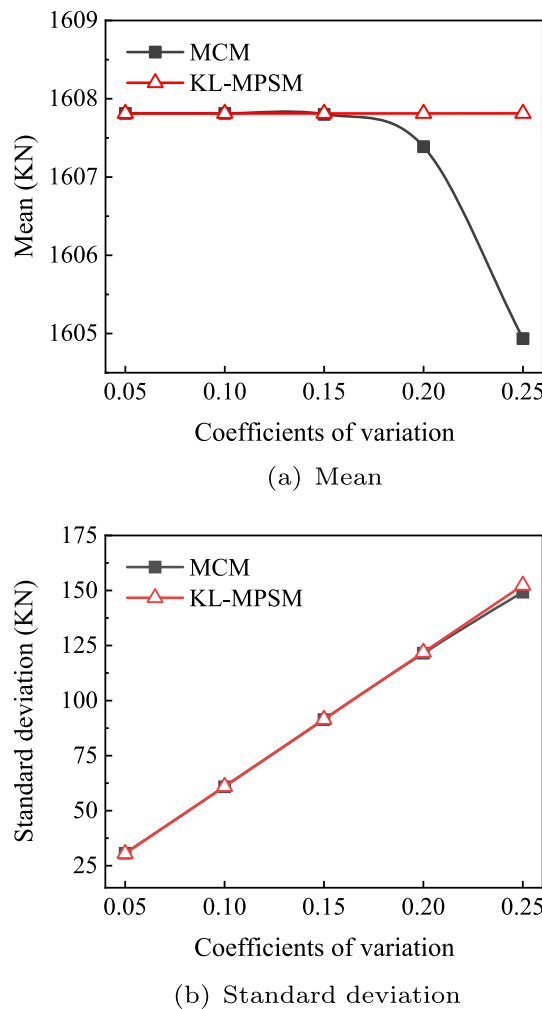


**Fig. 7** Mean and standard deviation of the structural resistance calculated by MCM and KL-MPSM with different coefficients of variation  $c_v$

According to the basic assumptions, plastic hinges only appear at nodes. Therefore, it is necessary to re-discretize the structure and add nodes at the midpoint of beams. In this example, it is assumed that the vertical uniform loads are permanent loads and do not change, and the horizontal load is applied step by step until the structure is destroyed. The ultimate horizontal load obtained finally is the ultimate

**Table 5** The reliability index and failure probability of the plane multilayer frame calculated by MCM and KL-MPSM with different coefficients of variation  $c_v$ 

$c_v$	MCM		KL-MPSM	
	Reliability index	Failure probability (%)	Reliability index	Failure probability (%)
0.05	1.886	2.964	1.888	2.951
0.10	0.946	17.216	0.930	17.617
0.15	0.635	26.256	0.605	27.274
0.20	0.475	31.736	0.437	33.099
0.25	0.371	35.538	0.333	36.954

load, that is, the structural resistance. The mean and standard deviation of  $R$  are shown in Fig. 7; the reliability index and failure probability are listed in Table 5.

In this example, PSM cannot compute the second-order estimates of the ultimate load, but KL-MPSM, due to its versatility, can handle this type of problem easily. The results further validate the previous viewpoint that KL-MPSM is an effective tool for static stochastic analysis in the case of low-level uncertainties.

## 7 Conclusion

In this paper, KL-MPSM is proposed, which combines the features of K–L expansion and MPSFEM for static stochastic analysis of structures with low-level uncertainties. Static stochastic analysis involves static stochastic computation and reliability analysis. In the reliability analysis, JC method is introduced to calculate the reliability index and failure probability by utilizing the second-order estimates obtained by KL-MPSM. The presented computational scheme is promoted to two directions, i.e., plane problems and plane frame structures, corresponding to two-dimensional random field and one-dimensional random field problems, respectively. In the numerical examples, the results obtained by MCM are treated as standard values to compare with KL-MPSM, and PSM is also introduced to verify the accuracy and efficiency superiorities of KL-MPSM. Therefore, conclusions are obtained as follows:

- (1) In the static stochastic analysis of structures with low-level uncertainties, KL-MPSM has an advantage over PSM in accuracy.
- (2) The programs of KL-MPSM can be done without character operations easily, and KL-MPSM can save a lot of CPU computation time compared to MCM.
- (3) KL-MPSM has a much broader scope of application than PSM and can be promoted to the stochastic analysis of a wide range of problems.

- (4) KL-MPSM is an effective tool for static stochastic analysis.

However, this paper also has shortcomings, such as the Gaussian assumption is not rigorous for the material elastic field [48–52]. Therefore, the main research direction in the subsequent work of KL-MPSM should be to promote it to deal with non-Gaussian random fields. For some simple non-Gaussian random fields, Refs. [21] and [22] can provide some basis; and for the case that the variables obtained by K–L expansion are generally dependent and defined by a probability measure that is unknown a priori, Wu provides a scheme for transforming correlated random variables into uncorrelated random variables [35]. The above ideas should be tried in the subsequent work.

**Acknowledgements** This work was funded by the National Natural Science Foundation of China (Grant No. 11972379), the Key R&D Program of Hunan Province (2020SK2060), Hunan Science Fund for Distinguished Young Scholars (2021JJ10061), and Open fund of State Key Laboratory of Hydraulic Engineering Simulation and Safety, Tianjin University.

## Declarations

**Conflict of interest** The authors declare they have no conflict of interests.

## References

1. Liu WK, Belytschko T, Mani A (1986) Random field finite elements. *Int J Numer Methods Eng* 23(10):1831–1845
2. Zhou H, Li J (2020) Energy-based collapse assessment of concrete structures subjected to random damage evolutions. *Probab Eng Mech* 60:103019
3. Wriggers P, Moftah SO (2006) Mesoscale models for concrete: Homogenisation and damage behaviour. *Finite Elem Anal Des* 42(7):623–636
4. Jiang L, Liu X, Xiang P, Zhou W (2019) Train-bridge system dynamics analysis with uncertain parameters based on new point estimate method. *Eng Struct* 199:109454
5. Liu X, Xiang P, Jiang L, Lai Z, Zhou T, Chen Y (2020) Stochastic analysis of train-bridge system using the Karhunen–Loève expansion and the point estimate method. *Int J Struct Stab Dyn* 20(02):2050025

6. Wang T, Zhou G, Wang J, Zhao X (2016) Stochastic analysis for the uncertain temperature field of tunnel in cold regions. *Tunn Undergr Sp Tech* 59:7–15
7. Li Z, Pasternak H (2019) Experimental and numerical investigations of statistical size effect in s235jr steel structural elements. *Constr Build Mater* 206:665–673
8. Wang X, Li Z, Wang H, Rong Q, Liang RY (2016) Probabilistic analysis of shield-driven tunnel in multiple strata considering stratigraphic uncertainty. *Struct Saf* 62:88–100
9. Wriggers P, Allix O, Weißenfels C (2000) *Virtual design and validation*. Springer, Berlin
10. Zein S, Laurent A, Dumas D (2019) Simulation of a gaussian random field over a 3d surface for the uncertainty quantification in the composite structures. *Comput Mech* 63:1083–1090
11. Rauter N (2021) A computational modeling approach based on random fields for short fiber-reinforced composites with experimental verification by nanoindentation and tensile tests. *Comput Mech* 67(2):699–722
12. Zakian P (2021) Stochastic finite cell method for structural mechanics. *Comput Mech* 68(1):185–210
13. Der Kiureghian A, Ke J-B (1988) The stochastic finite element method in structural reliability. *Probab Eng Mech* 3(2):83–91
14. Vanmarcke EMSGI, Shinozuka M, Nakagiri S, Schueller GI, Grigoriu M (1986) Random fields and stochastic finite elements. *Struct Saf* 3(3–4):143–166
15. Li C-C, Der Kiureghian A (1993) Optimal discretization of random fields. *J Eng Mech-ASCE* 119(6):1136–1154
16. Zhang J, Ellingwood B (1994) Orthogonal series expansions of random fields in reliability analysis. *J Eng Mech-ASCE* 120(12):2660–2677
17. Ghanem RG, Spanos PD (2003) *Stochastic finite elements: a spectral approach*. Courier Corporation, North Chelmsford
18. Sudret B, Der Kiureghian A (2000) *Stochastic finite element methods and reliability: a state-of-the-art report*. Department of Civil and Environmental Engineering, University of California, Berkeley
19. Zheng Z, Dai H (2017) Simulation of multi-dimensional random fields by Karhunen–Loève expansion. *Comput Methods Appl Mech* 324:221–247
20. Phoon KK, Huang SP, Quek ST (2002) Implementation of Karhunen–Loève expansion for simulation using a wavelet-Galerkin scheme. *Probab Eng Mech* 17(3):293–303
21. Kim H, Shields MD (2015) Modeling strongly non-gaussian non-stationary stochastic processes using the iterative translation approximation method and Karhunen–Loève expansion. *Comput Struct* 161:31–42
22. Tong M-N, Zhao Y-G, Zhao Z (2021) Simulating strongly non-gaussian and non-stationary processes using Karhunen–Loève expansion and l-moments-based hermite polynomial model. *Mech Syst Signal Process* 160:107953
23. Zhang D, Zhiming L (2004) An efficient, high-order perturbation approach for flow in random porous media via Karhunen–Loève and polynomial expansions. *J Comput Phys* 194(2):773–794
24. Montoya-Noguera S, Zhao T, Yue H, Wang Yu, Phoon K-K (2019) Simulation of non-stationary non-Gaussian random fields from sparse measurements using Bayesian compressive sampling and Karhunen–Loève expansion. *Struct Saf* 79:66–79
25. Blatman G, Sudret B (2011) Adaptive sparse polynomial chaos expansion based on least angle regression. *J Comput Phys* 230(6):2345–2367
26. Xiu D (2007) Efficient collocational approach for parametric uncertainty analysis. *Commun Comput Phys* 2(2):293–309
27. Kamiński M (2007) Generalized perturbation-based stochastic finite element method in elastostatics. *Comput Struct* 85(10):586–594
28. Kamiński M (2010) Potential problems with random parameters by the generalized perturbation-based stochastic finite element method. *Comput Struct* 88(7–8):437–445
29. Kamiński M (2009) Perturbation-based stochastic finite element method using polynomial response function for the elastic beams. *Mech Res Commun* 36(3):381–390
30. Kamiński M, Carey GF (2005) Stochastic perturbation-based finite element approach to fluid flow problems. *Int J Numer Methods Heat Fluid Flow* 15(7):671–697
31. Kamiński M, Solecka M (2013) Optimization of the truss-type structures using the generalized perturbation-based stochastic finite element method. *Finite Elem Anal Des* 63:69–79
32. Kamiński M, Kazimierzczak M (2014) 2D versus 3D probabilistic homogenization of the metallic fiber-reinforced composites by the perturbation-based stochastic finite element method. *Compos Struct* 108:1009–1018
33. Kamiński M, Hien TD (1999) Stochastic finite element modeling of transient heat transfer in layered composites. *Int Commun Heat Mass* 26(6):801–810
34. Kamiński M (2008) On stochastic finite element method for linear elastostatics by the Taylor expansion. *Struct Multidiscip Optim* 35(3):213–223
35. Feng W, Gao Q, Xiao-Ming X, Zhong W-X (2015) A modified computational scheme for the stochastic perturbation finite element method. *Lat Am J Solids Struct* 12:2480–2505
36. Wu F, Zhong WX (2016) A modified stochastic perturbation method for stochastic hyperbolic heat conduction problems. *Comput Methods Appl Mech Eng* 305:739–758
37. Liu X, Zhang Y, Li X, Xiang P, Xie S (2022) Running stability analysis for express wagon with modified stochastic perturbation method. In: *Second international conference on rail transportation*
38. Liu X, Xiang P, Jiang L, Lai Z, Zhou T, Chen Y (2020) Stochastic analysis of train-bridge system using the Karhunen–Loève expansion and the point estimate method. *Int J Struct Stab Dyn* 20(02):2050025
39. Grigoriu M (2010) Probabilistic models for stochastic elliptic partial differential equations. *J Comput Phys* 229(22):8406–8429
40. Rauter N (2021) A computational modeling approach based on random fields for short fiber-reinforced composites with experimental verification by nanoindentation and tensile tests. *Comput Mech* 67(2):699–722
41. Stefanou G (2009) The stochastic finite element method: past, present and future. *Comput Methods Appl Mech* 198(9–12):1031–1051
42. Liu Z, Yang M, Cheng J, Tan J (2021) A new stochastic isogeometric analysis method based on reduced basis vectors for engineering structures with random field uncertainties. *Appl Math Model* 89:966–990
43. Trinh M-C, Mukhopadhyay T (2021) Semi-analytical atomic-level uncertainty quantification for the elastic properties of 2d materials. *Mater Today Nano* 15:100126
44. Rackwitz R, Flessler B (1978) Structural reliability under combined random load sequences. *Comput Struct* 9(5):489–494
45. Choi KK, Kim N-H (2004) *Structural sensitivity analysis and optimization 2: nonlinear systems and applications*. Springer, Berlin
46. Hoang V-L, Dang HN, Jaspert J-P, Demonceau J-F (2015) An overview of the plastic-hinge analysis of 3d steel frames. *Asia Pac J Comput Eng* 2(1):1–34
47. Olsson A, Sandberg G, Dahlblom O (2003) On latin hypercube sampling for structural reliability analysis. *Struct Saf* 25(1):47–68
48. Soize C (2006) Non-gaussian positive-definite matrix-valued random fields for elliptic stochastic partial differential operators. *Comput Methods Appl Mech* 195(1–3):26–64
49. Grigoriu M (2016) Microstructure models and material response by extreme value theory. *SIAM-ASA J Uncertain Quantif* 4(1):190–217



50. Staber B, Guilleminot J (2017) Stochastic modeling and generation of random fields of elasticity tensors: a unified information-theoretic approach. *CR Mecanique* 345(6):399–416
51. Malyarenko A, Ostoja-Starzewski M (2017) A random field formulation of Hooke's law in all elasticity classes. *J Elast* 127(2):269–302
52. Guilleminot J (2020) Modeling non-gaussian random fields of material properties in multiscale mechanics of materials. In: *Uncertainty quantification in multiscale materials modeling*. Elsevier, pp 385–420

**Publisher's Note** Springer Nature remains neutral with regard to jurisdictional claims in published maps and institutional affiliations.

Springer Nature or its licensor (e.g. a society or other partner) holds exclusive rights to this article under a publishing agreement with the author(s) or other rightsholder(s); author self-archiving of the accepted manuscript version of this article is solely governed by the terms of such publishing agreement and applicable law.